

Application of Zenner-Frank Phase Field Theory for Simulating Cu Depletion Effect in Isothermally Aged SAC BGA Solder Joints

Naveen Daham Weerasekera, Ahmed Ijaz Abdulla

Abstract— In this paper, thermodynamic study of material transport in Pb free solder joint that is subjected to isothermal aging is performed. Thermodynamic feasibility is done through modeling the process by phase field method (PFM). Images of evolution of the experimental microstructure of the solder joint is accomplished by scanning electron microscopy (SEM) and optical microscopy (OM). Simulation results of the microstructure evolution and SEM images are compared for intermetallic compound Cu_6Sn_5 (IMC) of the solder joint. In the experimental investigations, we saw a depletion of IMC precipitates at the center of the solder joint matrix with isothermal aging. However, growth of the main IMC layer was investigated. Zenner-Frank theory of PFM is used to simulate the process with a simplified free energy density function. Initial precipitate distribution similar to experimental distribution is evolved with time and final microstructure with the experimental microstructure are compared. Phase field model soundly demonstrated the thermodynamic possibility of this process.

Index Terms— SAC Solder Joints, Scanning Electron Microscopy, Phase Field Modeling, Zenner-Frank theory, Precipitate Growth, Intermetallic Compounds, BGA Solder Joints .

1 INTRODUCTION

Research in Pb-free solder joints are on an increase of interest up to today's date. Advantages of these solder joints based on reduced environmental pollution and adverse health effects compared to Pb contained solder materials [1]. Alloy composition and grain structure of solder material plays a key role in determine its strength under various working conditions. Under these working conditions, isothermal aging can be considered as an important process. Since these conditions are prevalent in automobile and industrial applications [7]. Therefore, change in material composition and grain structure along with material migration is an important aspect of determining its strength [3].

Research in topology changes in Pb-free solder alloys subjected to isothermal aging are common. Formation of an IMC layer is desirable in the solder reflow process to produce a good bonding between solder metal and Cu substrate. However, a thick IMC layer can degrade the strength of the solder joint due to their inherent brittle nature [6]. One of the most common IMC compounds that can be found is the Cu_6Sn_5 . When in an individual element concentration identification process, high copper concentration is visible in this region compared to overall solder joint. Hung et al.[4] found that with the increase in Cu content, in the Sn-Cu solder joint samples, a large number of Cu_6Sn_5 particles distribute evenly in the matrix and

plays a role of joint strengthening. From the study performed by Lee [5], on flip-chip ball grid arrays (FCBGA) summarized the importance of investigation of these solder joints at elevated temperatures. Lee tested FCBGA solder joints subjected to impact and shock loading aged at elevated temperatures. Then the microstructure is studied. They concluded that 75°C, isothermal aging can be a stimulator to develop unstable Cu_6Sn_5 IMC that can degrade the shock performance. However, different isothermal aging conditions can be resulted in degradation or improvement of shock performance[5]. This paper presents a preliminary study to investigate feasibility of thermodynamic description for major material migration process in SAC solder joint. The thermodynamic study is performed through PFM targeting Cu migration in the solder matrix subjected to isothermal aging.

Xu et al. [2] discussed the atomic diffusion in SAC solder joints subjected to isothermal aging. Xu et al. observed the decrease in shear force under 600hours of aging time of SAC solder joint. From the test produced on Sn-Bi solder joints, the initial grain sizes of β -Sn and Sn-Bi bulks were enlarged. This enlargement considered as the main factor of reducing hardness of the joint. However, in their study, diffusing Cu into the middle of the solder joint acted as a hardening agent. Therefore, Xu et al. concluded that microstructure coarsening as a key factor for slight decrease in hardness [2]. During the material reflow process apart from the IMC layer formation, secondary precipitates of Cu_6Sn_5 and Ag_3Sn forms surrounding β -Sn dendrites that ultimately leads to Cu rich regions as in figure 1. The dominant role of Ag_3Sn over Cu_6Sn_5 precipitates in the strengthening of SAC solders is due to their prevalence and small size. The number density of the small

- Naveen Daham Weerasekera is currently pursuing Doctoral degree in material, thermal and fluid sciences at Portland State University, USA, Phone:+12674692310. E-mail: naveen@pdx.edu
- Ahmed Ijaz Abdulla obtained his bachelor's degree from National Institute of Technology, Silchar, INDIA, E-mail: ahmedijazabdulla@gmail.com

Ag_3Sn precipitates is a strong contributing factor to the enhancement of the creep and fatigue resistances of the SAC solder joints [8]. Microstructure studies of these IMC compounds are widely available in the literature. However, literature in modeling of migration of these compounds are scarce. In the scope of this paper we studied the diffusion process of Cu rich IMC (Cu_6Sn_5) subjected to interfacial conditions where multicomponent diffusion take place. Mookam et al. [9] studied the IMC layer growth process in SAC alloys with different Cu concentrations. They concluded that the diffusion coefficient of the solder joint is high when the Cu content of the solder increases, thereby correlating diffusion coefficient to Cu content in the solder material. Most importantly they reported the diffusion coefficients of Cu_6Sn_5 IMC for Sn-0.7Cu, Sn-1.0Cu and Sn-3.0Cu are providing a good support for current study. Present literature has a scarcity in the area of introducing modeling of transport of these IMCs in the solder matrix subjected to interfacial gradients. Therefore, a modeling method has to be identified to visualize the process without an experimental process, however, the model has to be validated by real data before it is implemented. We are given an attempt to achieve this goal by this work.

When modeling the process of material transport in the solder matrix, interfacial diffusion is certain to account. The microstructure of the matrix is based on its distribution and minimization of free energies of individual components. This is called the spinodal decomposition where enlargement of the grains takes place. Therefore, an application of a model that accounts these properties are necessary. PFM provides the accessibility to model interfacial diffusion processes and microstructure evolution of multicomponent mixtures [10]. Studies on precipitate growth using PFM are widely available in the literature. Fleck et al. presented PFM of precipitate growth in Ni based alloys subjected to industrial heat treatments [11]. They introduced the necessary parameters such as length and time scaling and interfacial parameters (Atomic Mobility etc.) and methodology of implementing thermal processes for such simulations that helps to create a basis for the simulations in this study. Proving further support for current work, Chen et al. [12], performed diffusion-controlled precipitation growth on Ti-Al-V alloys. They provided the pathways to implementing different mobility parameters of diffusion using assessed databases. Furthermore, Han et al. [13] performed studies in precipitate growth in Mg-Al alloys subjected to aging by applying diffuse interface model which is also applied in our work. They also highlighted the effect of the mobility parameter on the diffusion process. Furthermore, Zhang et al. [14] introduced the important process of identifying material parameters by phase field modeling and experiments. They used experimental microstructure as the initial parameter and evolved it through time. They performed a largely similar process as we done in this study, by comparing experimental

and simulated microstructures to obtain liquid diffusion parameters of Al-Cu alloy.

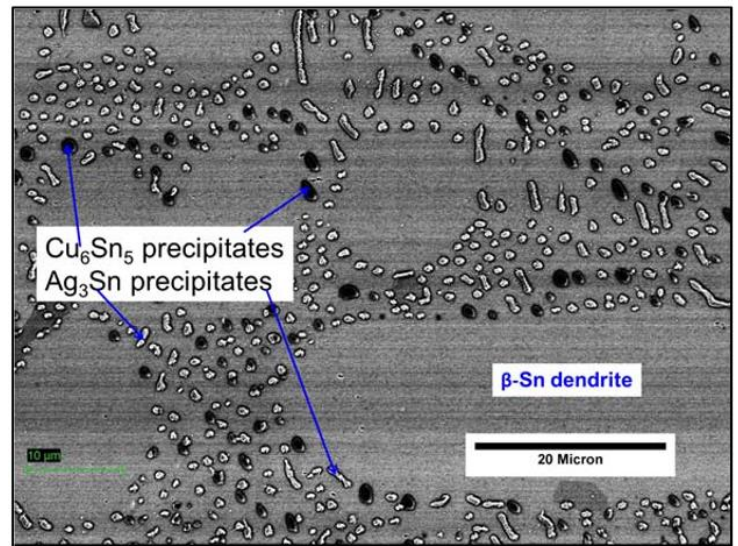


Figure 1: SEM micrographs of intermediate Cu_6Sn_5 and Ag_3Sn precipitates formed in the middle of the solder joint (Courtesy: Mutuku et al. [8])

This study is performed to investigate thermodynamic process transport of Cu present in IMC regions in the solder joint by PFM. Microstructure can be attributed to a thermodynamically unstable structure that evolves with time to find its stability. PFM became a powerful method to identify the mechanism of microstructure evolution specifically in precipitation growth and grain growth pertaining to current study. The basic model of phase field equations are based on set of partial differential equations which are solved numerically. In these equations different driving forces of microstructural evolution such as minimization of bulk free energy, elastic energy, and interfacial energy are considered. In general, these equations are based on thermodynamic and kinetic properties [15]. From this overview, PFM can be applied to validate an experimental microstructure from its theoretical counterparts. The analysis of this paper is carried out from the Zenner-Frank (ZF) phase field theory, since the theory has extended to study diffusional growth problems in variety of settings [16]. ZF theory is widely used for simulating precipitate growth by adopting their thermodynamic and kinetic properties [16]. Due to these properties of ZF theory, we concluded that it is relevant to model current phenomena by it based on the experimental microstructures available.

2 ANALYSIS

In this analysis, cross section of a single solder joint is simulated through PFM. In figure 1, the optical micrograph of the cross section of the solder joint depict basic distribution of Sn and Cu rich regions. The package size of the sample is 12×12 mm and 0.5mm pitch with 228IOs.

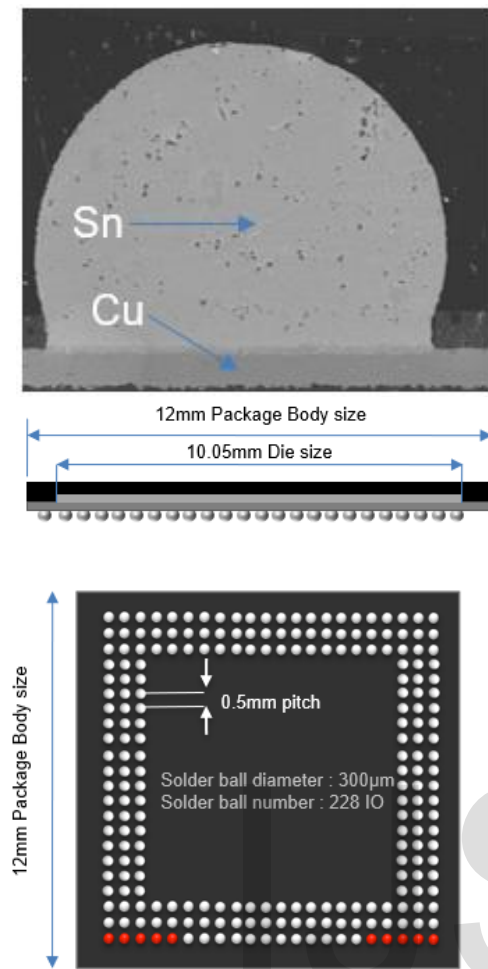


Figure 2: Top: Solder joint cross section, Bottom: Typical application in a package

2.2 Experimental Microstructure

2.2.1 Experimental Process

SAC solder joint used herein are placed on OSP (organic surface preservative) surface finish. Unlike Ni-Au surface finish, solder joints with OSP surface finish produces Cu_6Sn_5 and Ag_3Sn restrictively rather than Ni based IMCs. Four similar electronic packages containing solder joints are placed in the Despatch, RAD cabinet oven separately at 150°C for 50hr, 100hr, 150hr and 500hr. After aging, packages are dipped in a transparent epoxy resin and allowed to solidify. These samples are then smoothly grinded to the middle of the nearest single joint bead from the package edge. These sections are then studied by scanning electron microscopy (SEM) and experimental microstructure is obtained. SEM images of cross sections of solder joints are given in figure 3.

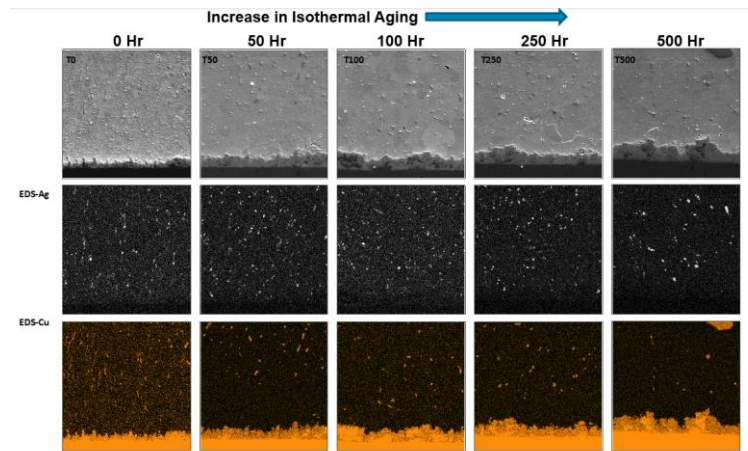


Figure 3: Experimental micrographs of Cu and Ag microconstituents of aged samples. From columns from left to right: 50hr, 100hr,150hr, 250hr, 500hr.

3 PHASE FIELD MODELING

Phase field modeling is carried out using a customary developed MATLAB code. The model is reduced to 2D without losing mandatory information of the microstructure. In the model, Cu phase is initially randomly distributed in the entire solder joint as in figure 3. Also, in figure 3, the Cu dense area where the Cu_6Sn_5 IMC lies, is depicted as a dense strip of Cu. From its basic understanding of PFM, the stability of initial microstructure is determined by the thermodynamic and kinetic properties. By time evolving this microstructure at a specific temperature or and external condition, system gains its most stable form. This property is related to current study through evolving microstructure in specific background temperatures. In isothermal aging of the initial microstructure of solder joint at specific temperatures stands in search for its most stable microstructure at that temperature. This is based on minimizing its free energy functional (FEF) (Gibbs free energy, diffusion properties) pertaining to that temperature. Therefore, for each different temperature, the control parameters of the FEF has to be altered. However, in this study, we considered all parameters that are part of the FEF as unity for simplicity. Since the objective of this paper is to get a rough estimate of microstructure evolution, this action is taken. Therefore, the model is evolved to its climax where no more microstructure change is visible, is considered as the stable microstructure. This stable microstructure is obtained after 50s of simulation time with minor variations greater than 50s. This evolution is monitored intermediately and shown in figure 6 to 9. It is important to note that figures 6 and 7 are contoured based on PFM order parameter. This order parameter is representing individual Cu_6Sn_5 . Figures 8 and 9 are contoured based on composition order parameter that is normalized Cu concentration at its mother solution (Cu_6Sn_5).

3.1. Formulation

In this phase field model, we simulated the process through considering a binary alloy at constant temperature where isolated precipitate of Cu_6Sn_5 phase grows into the matrix phase of β -Sn. There are two order parameters based on composition (c) and microstructure (η). The normalized condition is based on at Cu_6Sn_5 phase $\eta=1$ and Sn phase $\eta=0$. Also, composition is following the same rule, however, based on phase Cu chemical composition, considering $c = 1$ at Cu_6Sn_5 phase and $c = 0$ at β -Sn phase.

The microstructure evolution of the system is given by Cahn-Hilliard (1) and Alan-Chan (2) equations [3] as,

$$\frac{\partial c}{\partial t} = \nabla \cdot M \nabla \mu \tag{1}$$

$$\frac{\partial \eta}{\partial t} = -L \frac{\delta(F/N_v)}{\delta \eta} \tag{2}$$

Where, M is the atomic mobility, μ is the chemical potential and L is the relaxation coefficient for the order parameter. Chemical potential μ is defined as the variational derivative of the total free energy per atom F with respect to the local composition c .

$$\mu = \frac{\delta(F/N_v)}{\delta c} \tag{3}$$

The total free energy F of the system is given by the sum of chemical free energy F^{ch} and elastic free energy F^{el} . However, for this model, we only use chemical free energy of precipitate growth since elastic properties are not in interest. Therefore, the chemical contribution for the total free energy is given as a functional of composition (c) and microstructure (η) order parameters as,

$$F^{ch} = N_v \int_{\Omega} [f(c, \eta) + \kappa_c (\nabla c)^2 + \kappa_{\eta} (\nabla \eta)^2] d\Omega \tag{4}$$

Where, $f(c, \eta)$ is the bulk free energy per atom and κ_c is the gradient energy coefficient for the composition order parameter and κ_{η} is that for the microstructure order parameter. Where, N_v is the number of atoms per unit volume. Bulk free energy density $f(c, \eta)$ is given by,

$$f(c, \eta) = f^m(c)(1 - W(\eta)) + f^p(c)W(\eta) + P \cdot \eta^2(1 - \eta)^2 \tag{5}$$

In equation (5), $f^m(c)$ is the free energy of the matrix phase and $f^p(c)$ is that of the precipitate phase. These two free energy functions can be given by following simple forms as [3],

$$f^m(c) = Ac^2 \tag{6}$$

$$f^p(c) = B(1 - c)^2 \tag{7}$$

Where, A and B are positive constants. The values of these constants are decided based on the temperature where these free energy functions are considered. Figure 4 and 5 represents the simple plots of these free energy density functions with two different A and B values. The intersection of the curves of $f^m(c)$ and $f^p(c)$ gives the stable form or the possible minimum free energy at the considering temperature. In addition, the overall free energy curve is the union of individual curves of $f^m(c)$ and $f^p(c)$ at constant temperature [16].

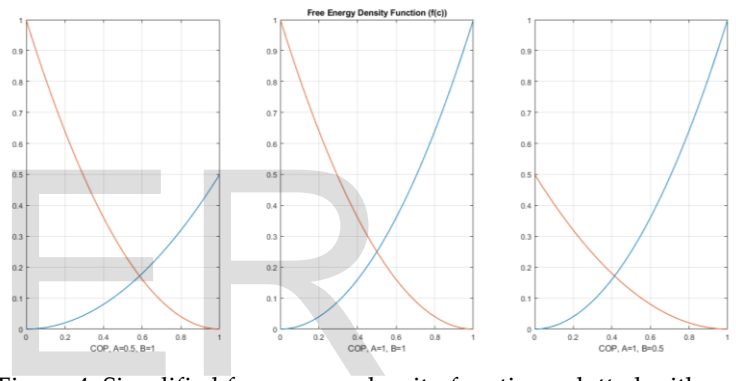


Figure 4: Simplified free energy density functions plotted with respect to composition order parameter (COP) for different A and B values.

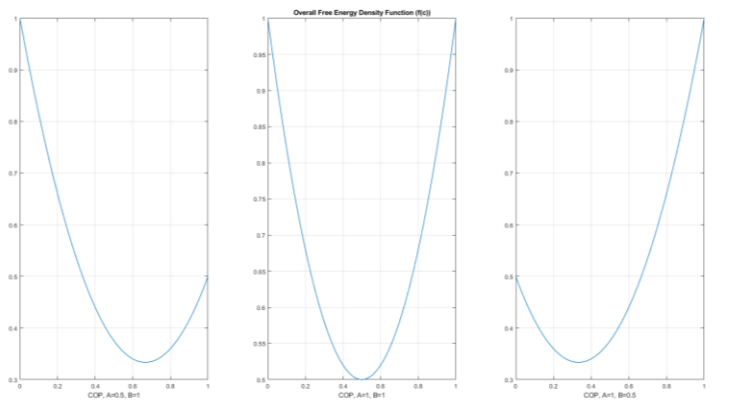


Figure 5: Plot of the combination of $f^m(c)$ and $f^p(c)$ provides the complete simplified free energy density function

$W(\eta)$ is the interpolation function which is known as the Wang function [16] which is given as a piecewise polynomial of η as,

$$\begin{aligned}
 W(\eta) &= 0 && \text{for } \eta < 0, \\
 W(\eta) &= \eta^3(10 - 15\eta + 6\eta^2) && \text{for } 0 \leq \eta \leq 1 \\
 W(\eta) &= 1 && \text{for } \eta > 1
 \end{aligned}
 \tag{8}$$

Finite difference method is used to discretize the governing equations (1) and (2). For simplicity the system is considered as sufficiently large therefore, the periodic boundary conditions are implemented [17]. The grid size used was 128×128 after optimizing the grid size from the grid independence study.

4 SIMULATION RESULTS

Simulation as are performed from the scaled time frame using MATLAB software. Since, the initial microstructure obtains its most stable microstructure in the isothermal process the simulation time can be accurately scaled. Therefore, simulation mainly depends on Gibbs free energy density function defined at respective isothermal temperature. Figure 6 represents the initial microstructure before the simulation. This microstructure is applied parallel to the SEM micrographs. Since periodic boundary conditions are applied, to avoid the edge effect, main IMC layer is shifted upwards by 20 Y- grid points. Therefore, growth of the main IMC layer towards both positive and negative directions can be observed. Figures 7 and 8 presents the evolution of the microstructure order parameter up to 50s. And figures 9 and 10 represents the evolution of composition order parameter also up to 50s.

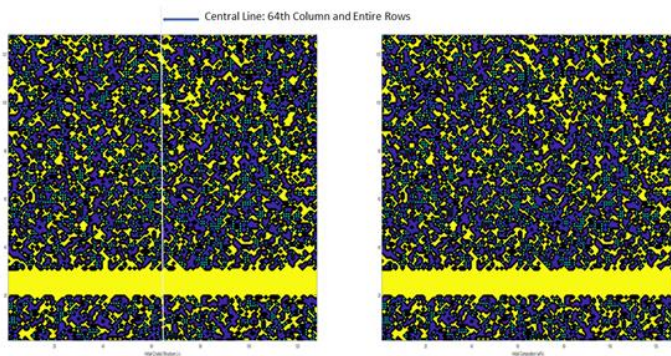


Figure 6: Initial microstructure (left) and composition (right) order parameter distribution before simulation (Contour plot range: 0 to1, X and Y axes are grid points)

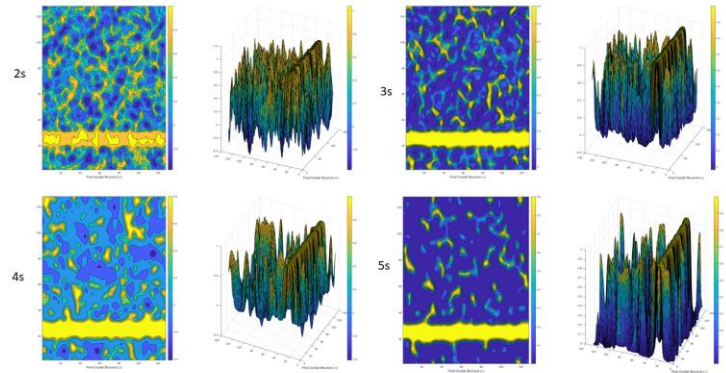


Figure 7: Evolution of microstructure from 2s to 5s (Contour plot range: 0 to1, X and Y axes are grid points)

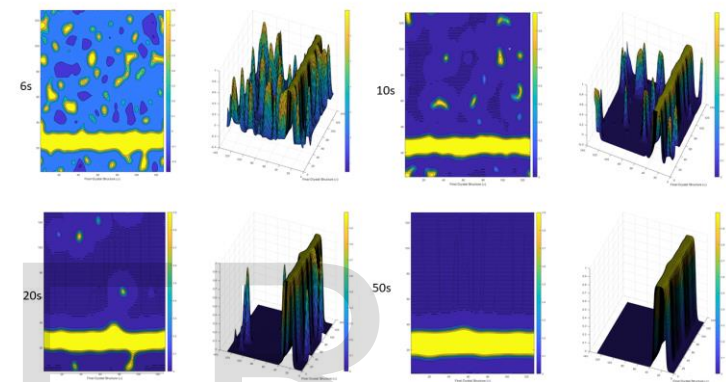


Figure 8: Evolution of microstructure from 6s to 50s (Contour plot range: 0 to1, X and Y axes are grid points)

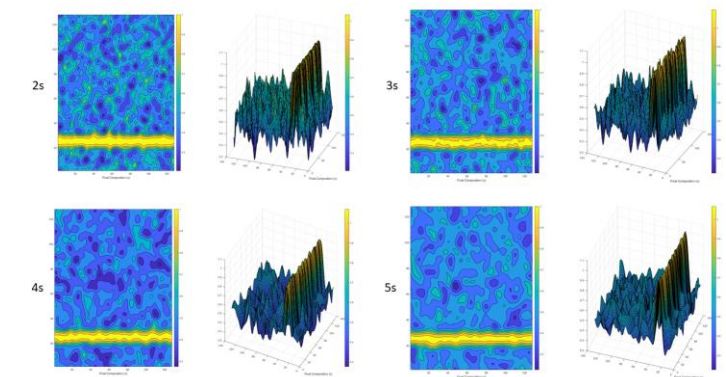


Figure 9: Evolution of composition from 2s-5s (Contour plot range: 0 to1, X and Y axes are grid points)

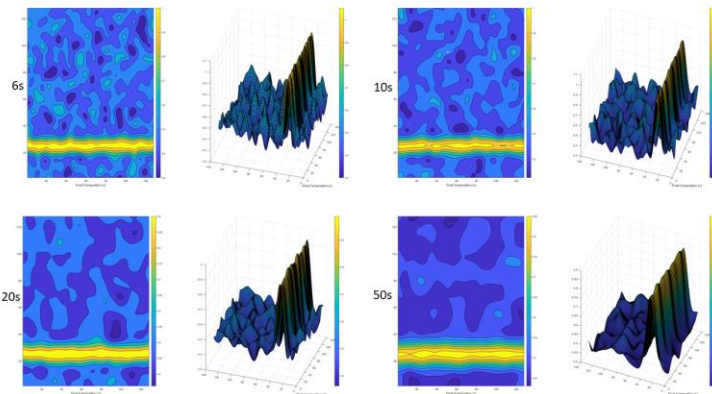


Figure 10: Evolution of composition from 6s-50s (Contour plot range: 0 to 1, X and Y axes are grid points)

To clearly visualize precipitate depletion and IMC layer growth, graphs are plotted for microstructure order parameter against central nodal distance located as in figure 6. Figures 11 and 12 represent variation of microstructure in this central node line up to 50s.

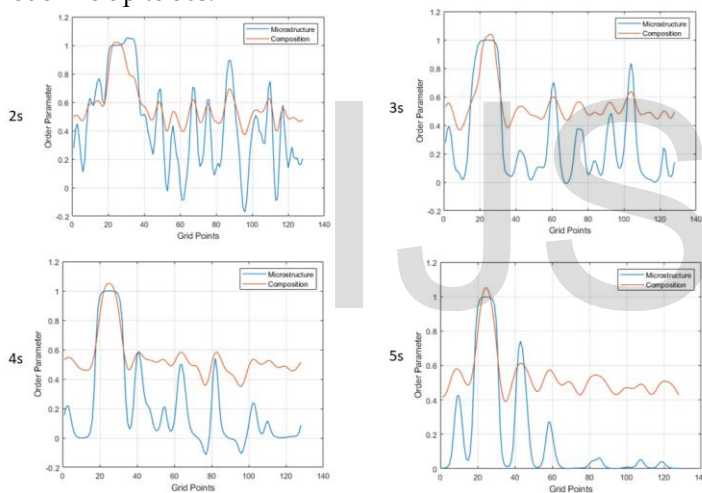


Figure 11: Order parameter variation at a central node line (in figure 6) from 2s to 5s (X- axis: grid points, increasing to positive x-direction, Y-axis: value of the microstructure order parameter (0-1))

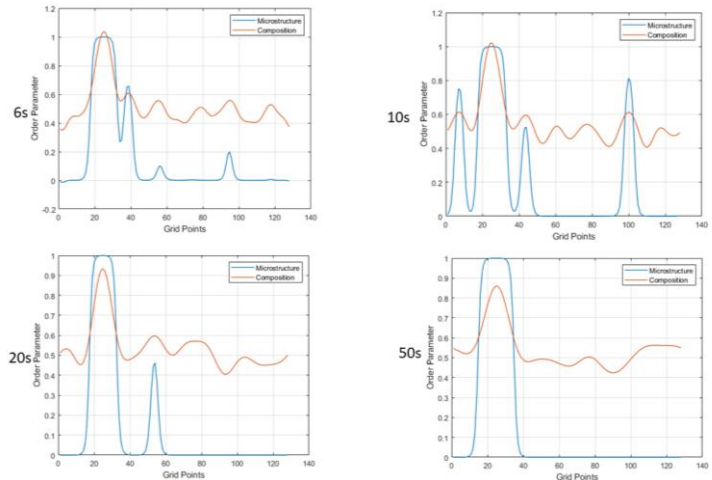


Figure 12: Order parameter variation at the central node line (as in figure 6) from 6s to 50s (X- axis: grid points, increasing to positive x-direction, Y-axis: value of the microstructure order parameter (0-1))

5 DISCUSSION

When investigating experimental microstructure, initially Cu is distributed randomly at a high concentration throughout the solder joint. These distributions can be categorized as Cu precipitates apart from the Cu present in the Cu_6Sn_5 IMC at the bottom. In the subsequent aging process up to 500hrs, those Cu precipitates do not grow at their locations, but they are transported through the entire compound matrix to the Cu rich region (Cu_6Sn_5 , IMC). This process is apparent in the microstructure, as the IMC layer is growing with the aging process, however, overall Cu precipitates are reducing in the middle of the solder joint.

As another evidence for this process, Cu concentration at the IMC layer increased depicting higher order parameter greater than 1. This occurrence is possible also due to the Gibbs-Thompson effect [3]. However, considering the overall process comparing with other regions of the matrix, we can still conclude the growth of the IMC layer.

In PFM, this process is clearly simulated. In low time evolutions such as from 2s to 20s the precipitates at the middle of the joint are getting depleted. However, Cu dense area depicted in figure 3, tends to grow towards the middle of the joint.

Therefore, it is identifiable that Cu is trying to accumulate in the Cu rich region. After accumulation is complete, isolated Cu region grows like a normal precipitate. Comparable to the experimental microstructure at 500hrs of aging, the distribution of random Cu precipitates in the middle of the matrix is demonstrated by multiple peaks of composition order parameter in the middle of the matrix in figure 9, 50s of time evolution.

6 CONCLUSION

In this paper Cu migration and depletion is studied using phase field modeling. Depletion of Cu precipitates distributed in the center of the solder joint reduces the overall strength of the joint. Depletion is caused by isothermal aging where microstructure regains its most stable form based on thermodynamics between phases. Phase field model clearly demonstrated this phenomena. Therefore, such phase field models based on Zener-Frank field theory is useful in predicting in precipitate behavior in such solder joints made from SAC alloys.

ACKNOWLEDGMENT

The authors wish to thank Dr. Agnimitra Biswas of Department of Mechanical Engineering of National Institute of Technology, Silchar for his constant motivation and support

REFERENCES

- [1] Jianbio Pan, David Shaddock, Jyhwen Wnag, "Lead free solder joint reliability – state of art and perspectives", *Journal of Microelectronics and Electronic Packaging*, Vol 2, No.1, 2005
- [2] Ruisheng Xu, Yang Liu, Fenglian Sun, "Effect of isothermal aging of the microstructure, shear behavior and hardness of the Sn58Bi/Sn3.0Ag0.5Cu/Cu solder joints", *Results in Physics*, 15(2019) 102701
- [3] Meng Zhao, Liang Zhang, Zhi Quan Liu, Ming Yu Xiong, Lei Sun, "Structures and properties of Sn-Cu lead free solders in electronic packaging", *Science and Technology of Advanced Materials*, 2019, Vol 20, No1. 421-444
- [4] Hung F, Lui T, Chen L, et al. Resonant characteristics of the microelectronic Sn-Cu solder. *J Alloys Compd.* 2008;457(1-2):171-176.
- [5] Tae Kyu Lee, "Impact of External Temperature Environment on Large FCBGA Sn-Ag-Cu Solder Interconnect Board Level Mechanical Shock Performance", *Journal of Welding and Joining*, Vol. 32, No.3, 2014
- [6] Liu Mei Lee, Ahmad Azmin Mohamad, "Interfacial Reaction of Sn-Ag-Cu Lead-Free Solder Alloy on Cu: A Review", *Advances in Material Sciences and Engineering*, (2013)
- [7] I.E. Anderson, J.L.Harringa, "Elevated Temperature Aging of Solder Joints Based on Sn-Ag-Cu: Effects on Joint Microstructure and Shear Strength", *Journal of Electronic Materials*, Vol 33, No. 12, 2004
- [8] Francis M. Mutuku, Babak Arfaei, Eric Cotts, "Effects of composition and isothermal aging on the microstructure and performance of alternate alloy Pb-free solder joints", *Proceedings of SMTA International*, 2016
- [9] N Mookam, P Tunthawiroon, K Kanlayasiri, "Effects of copper content in Sn-based solder on the intermetallic phase formation and growth during soldering", *Materials Science and Engineering*, 361 (2018), 012008
- [10] R.R.Mohanty, Y.Sohn, "Phase-Field Investigation of Multicomponent Diffusion in Single-Phase and Two-Phase Diffusion Couples", *Basic and Applied Research*, (2006) 27:676-683
- [11] Michael fleck, Felix Schleifer, Markus Holzinger, Uwe Glatzel, "Phase-Field Modeling of Precipitation Growth and Ripening During Industrial Heat Treatments in Ni-Base Superalloys", *The Minerals, Metals & Materials Society and ASM International 2018*"
- [12] Qing Chen, Ning Ma, Kaisheng Wu, Yunzhi Wang, " Quantitative phase field modeling of diffusion controlled precipitate growth and dissolution in Ti-Al-V", *Scripta Materialia*, 50 (2004) 471-476
- [13] G M Han, Z Q Han, A A Luo, A K Sachdev, B C Liu, "Phase field simulation of precipitation in a Mg-Al alloy using two techniques of approximation", *IOP Conf. Series: Materials Science and Engineering* 33 (2012) 012110"
- [14] Shu-zhou ZHANG^a, Rui-jie ZHANG, ^aXuan-huiQU, ^{ab}Wei FANG, ^aMing-zhi LIU^a, "Phase field simulation for non-isothermal solidification of multicomponent alloys coupled with thermodynamics database", *Transactions of Nonferrous Metals Society of China*, Vol. 23, 8, 2013: 2361-2367
- [15] Nele Moelans, Bart Blanpain, Patrick Wollants, "An introduction to phase field modeling of microstructure evolution", *Computer Coupling of phase Diagrams and Thermochemistry*, 32(2008) 268-294
- [16] R. Mukerjee, T.A. Abinandan, M.P. Gururajan, "Phase field study of precipitation growth: Effects of misfit strain and effects of curvature", *Acta Materialia*, 57(2009) 3947-3954
- [17] I. Muench, A. Renuka Balakrishna, J.E. Huber, "Periodic boundary conditions for the simulation of 3D domain patterns in tetragonal ferroelectric material", *Archive of Applied Mechanics*, (2019) 89: 955-972